Available online at www.sciencedirect.com
SCIENCE DIRECT®
Journal of Solid State Chemistry 177 (2004) 4800–4805
JOURNAL OF SOLID STATE CHEMISTRY
www.elsevier.com/locate/jssc

Rapid communication

Synthesis, characterization, and catalytic properties of stable mesoporous molecular sieve MCM-41 prepared from zeolite mordenite

Shan Wang[a], Tao Dou[a,b,*], Yuping Li[a], Ying Zhang[b], Xiaofeng Li[a], Zichun Yan[a]

[a] *Institute of Special Chemicals, Catalysis and Porous Materials Di, Taiyuan University of Technology, No. 79 West Yingze Street, Taiyuan City, ShanXi Province 030024, PR China*
[b] *The CNPC key laboratory of Catalysis, University of Petroleum, Fuxue Road, Changping, Beijing 102249, PR China*

Received 9 August 2004; received in revised form 1 October 2004; accepted 5 October 2004

Abstract

Mesoporous molecular sieves (denoted as M-MCM-41) with ordered hexagonal structure have been successfully synthesized from the assembly of precursors from preformed zeolite Mordenite with CTAB surfactant micelle in alkaline media. The samples were characterized by XRD, N_2 adsorption, IR and DTG. The materials exhibit highly hydrothermal stability, as compared with conventional MCM-41. Characterization results indicate that the mesoporous walls of M-MCM-41 contain the secondary building units similar to those in microporous crystal of zeolite Mordenite. In catalytic dealkylation of $C10^+$ aromatic hydrocarbon, M-MCM-41 shows higher activities in comparison with Mordenite and MCM-41, which would be ascribed to the combination of advantages of both MCM-41 (large pores) and Mordenite (strong acidity). Furthermore, this synthesis strategy could be used as a new general method for the preparation of hydrothermally stable mesoporous aluminosilicate materials under alkaline conditions.

Keywords: Mesoporous molecular sieve; Synthesis; Characterization; MCM-41; M-MCM-41

1. Introduction

Mesoporous molecular sieves such as MCM-41 have attracted much attention because of their potential use as versatile catalysts and catalyst supports for the conversion of large molecules [1]. However, as compared with conventional zeolites, these mesostructured materials have relatively low acidity and hydrothermal stability, which can be attributed to the amorphous nature of the mesopore walls [1,2]. Many efforts have been made to improve the hydrothermal stability and acidity of mesoporous materials. Researchers expect to improve both the stability and acidity of mesoporous materials [3–9] by introducing zeolite structure building units into the pore walls. There have been some successful examples of the preparation of mesoporous aluminosilicates that have reasonably good hydrothermal stability and strong acidity by the assembly of zeolite seeds solution or preformed aluminosilicate nanoclusters with surfactants such as CTAB in alkaline media [10,11] or triblock copolymer in acidic media [12]. For examples, Pinnavaia et al. reported the synthesis Al-MSU-S assembled from a zeolite type Y seeds solution [13], a zeolite Beta seeds solution [14,15], and a zeolite MFI seeds solution [14,15]; Xiao et al. reported mesoporous materials of MAS-7 [16], MAS-9 [12] and MTS-9 [17] assembled from preformed nanosized Beta, MFI, and TS-1 precursors, respectively. All of these

*Corresponding author. Institute of Special Chemicals, Catalysis and Porous Materials Di, Taiyuan University of Technology, No. 79 West Yingze Street, Taiyuan City, ShanXi Province 030024, PR China. Fax: +86 351 6010311.
E-mail address: dtao1@yeah.net (T. Dou).

0022-4596/$ - see front matter © 2004 Elsevier Inc. All rights reserved.
doi:10.1016/j.jssc.2004.10.010

mesoporous materials show highly hydrothermal stability and good activity in catalytic conversion of organic compounds, as compared with conventional mesoporous materials such as MCM-41 and SBA-15. Until more recently Ying et al. have successfully prepared zeolites with M41S mesostructure via hydrothermal treatment of different M41S-type materials at different pH, duration, and temperatures [18], the preparation of such mesopores from preformed zeolites remains an untouched area. Based on the similar concept, an alternative approach for the preparation of hydrothermally stable mesoporous aluminosilicates with strong acidity is reported in this paper.

Recently we have successfully synthesized a kind of hydrothermally stable mesoporous molecular sieve by using zeolite Mordenite as silica-alumina source. Zeolite Mordenite was dissolved into alkaline solutions by controlling the PH value and the dissolution time. There was a large number of secondary building units characteristic of zeolite Mordenite besides the completely dissolved silica source. With the addition of surfactant CTAB, the dissolved Mordenite gel would condense around the self-assembling aggregate of CTAB and many secondary building units in the initially dissolved aluminosilicate could be introduced into the mesopore walls. In this paper, the materials were thoroughly characterized by means of X-ray diffraction (XRD), nitrogen adsorption–desorption isotherm measurements, infrared (IR) spectroscopy and differential thermogravimetric (DTG) analysis. Catalytic activity in the dealkylation of $C10^+$ aromatic hydrocarbon has been investigated using the new mesoporous molecular sieve. Our results show that the new material synthesized from the preformed zeolite Mordenite is hydrothermally stable, and the catalytic activity of the new material is superior over conventional material MCM-41.

2. Experimental

2.1. Synthesis

The hydrothermally stable mesoporous sample was prepared using zeolite Mordenite as silica-alumina source. A typical synthesis procedure of the sample (denoted as M-MCM-41, for clarity) was as follows: 3.15 g of zeolite Mordenite (SiO_2/Al_2O_3 ratio is 30) was dispersed in 20 mL of a solution of sodium hydroxide (NaOH, 3.5 M aqueous solution) and stirred for 30 min at room temperature. To this solution was added 40 g solution of hexadecyltrimethylammonium bromide (CTAB, 16 wt% aqueous solution). After additional stirring for about 30 min the mixture was transferred into stainless-steel autoclaves for hydrothermal treatment at 373 K for 24 h. After cooling to room temperature, the PH value of the reaction mixture was adjusted to 8.5 by dropwise addition of 2 M HCl solution with vigorous stirring. The mixture was then loaded into an autoclave and heated at 373 K for 24 h at autogenous pressure again. The autoclave was quenched with cold water to stop the crystallization process. The solid product was recovered by filtration, washed with deionized water, dried in air at 353 K. The as-synthesized product was calcined at 823 K in air for 6 h using a muffle furnace. The NH_4^+ form of samples were obtained by repeated ion exchange with 1 M NH_4NO_3 solution for 2 h at 343 K. The protonated form was then obtained by calcining the NH_4^+ form at 773 K for 5 h.

For comparison, a MCM-41 sample with the SiO_2/Al_2O_3 ratio of 30 was synthesized under exactly the same conditions as M-MCM-41 sample except that the alkaline solution of Mordenite was replaced by a corresponding amount of TEOS (tetraethyl orthosilicate) and aluminum isopropoxide.

2.2. Characterization

XRD patterns of the samples were recorded using a Rigaku D/max-2500 X-ray powder diffractometer, which employed Ni-filtered Cu$K\alpha$ radiation and was operated at 40 kV and 100 mA. The nitrogen adsorption and desorption isotherms at 77 K were measured using a Micromeritics ASAP2010 system. The pore-size distribution for mesopore was analyzed from the desorption branch of the isotherm by the Barrett–Joyner–Halenda (BJH) method. IR spectra of the samples were recorded on a BIO-RAD FT-IR spectrometer (FTS165) with a resolution of 2 cm^{-1}. DTG analysis was performed on a Netzsch STA409C thermal analyzer.

2.3. Catalytic tests

Catalytic tests for the dealkylation of $C10^+$ aromatic hydrocarbon were carried out using a conventional flow reactor, and the analyses of the catalytic products were carried out with an SP-2100 gas chromatograph (Beijing Analytic Instrumental Co.) equipped with an FID detector. The catalytic reaction was performed according to the following standard conditions: the mass catalyst was 0.4996 g; reaction temperature and pressure were 823 K and 5.0 MPa, respectively; the amount of reaction products was 0.5 mL/h.

3. Results and discussions

3.1. X-ray diffraction (XRD)

Fig. 1 shows XRD patterns of as-synthesized, calcined, and treated M-MCM-41 and MCM-41 sam-

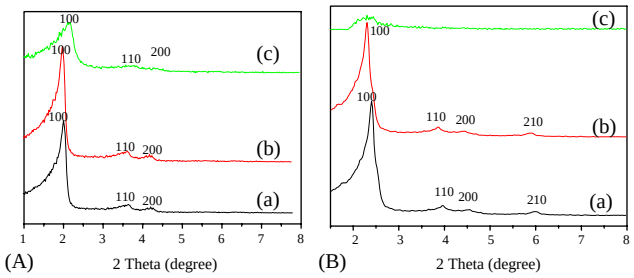

Fig. 1. XRD patterns of: (a) as-synthesized, (b) calcined and (c) treated (A) M-MCM-41 and (B) MCM-41. Treated M-MCM-41 in boiling water for more than 96 h; treated MCM-41 in boiling water for 24 h.

ples. The M-MCM-41 sample shows three resolved peaks (Fig. 1A(a)) that can be basically indexed as (100), (110), and (200) reflections associated with the hexagonal symmetry. The (100) peak reflects a d spacing of 4.52 nm. No diffraction peak was observed in the region of higher angles (8–35°), which indicates the absence of large crystals in the sample, suggesting that M-MCM-41 sample is a pure phase.

It is very interesting to note that the d(100) value of M-MCM-41 is much larger than that of MCM-41 prepared from the same condition. Furthermore, it is notable that M-MCM-41 is not as ordered as MCM-41. The XRD pattern shows that M-MCM-41 exhibits only three resolved peaks, while MCM-41 gives rise to four well-resolved peaks. It is proposed that this phenomenon could be attributed to the differences between the secondary building units from zeolite Mordenite used for M-MCM-41 and the non-structure silicate-alumina species used for MCM-41. The stronger rigidity and larger volume of the Mordenite units from the preformed zeolite make it relatively difficult to assemble with the template, resulting in some disorder in the M-MCM-41 sample.

After calcination in air at 823 K for 6 h, the XRD pattern of M-MCM-41 (Fig. 1A(b)) shows that the three diffraction peaks are still present, confirming that the hexagonal M-MCM-41 is thermally stable. Particularly, after treatment of calcined M-MCM-41 in boiling water for more than 96 h (Fig. 1A(c)), its XRD pattern still shows those peaks assigned to the hexagonal symmetry. In contrast, after treatment of the calcined MCM-41 in boiling water for 24 h, its mesostructure is almost destroyed completely (Fig. 1B(c)). These results indicate that the M-MCM-41sample has much higher hydrothermal stability than conventional MCM-41.

3.2. N_2 adsorption–desorption isotherms

Fig. 2 shows N_2 adsorption–desorption isotherms of calcined M-MCM-41 and MCM-41. Both samples give typical type-IV isotherms with a sharp inflection at relative pressure $P/P_0 > 0.3$, characteristic of capillary

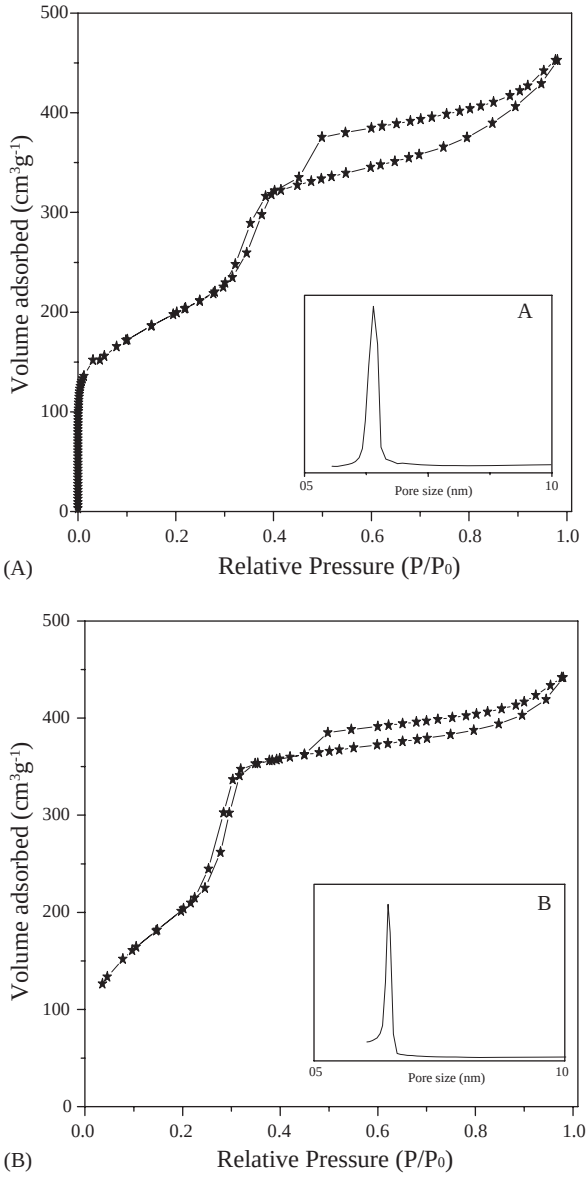

Fig. 2. Nitrogen adsorption–desorption isotherms and pore size distribution curves (inset) of calcined (A) M-MCM-41 and (B) MCM-41.

condensation, which indicate the uniformity of the mesopore size distribution. Notably, The pore size of M-MCM-41 (2.78 nm) and MCM-41 (2.95 nm) is similar, but the wall thickness is quite distinguishable, giving at 2.44 and 1.40 nm for M-MCM-41 and MCM-41, respectively (Table 1). Clearly, the wall thickness of M-MCM-41 assembled from preformed zeolite Mordenite precursors is much larger than that of MCM-41. This phenomenon is all assigned to that the Mordenite secondary building units used in the synthesis of the M-MCM-41 has stronger rigidity and larger volume than those non-structure silica-alumina species used in conventional synthesis of MCM-41, therefore, the assembly of these secondary building units need more

Table 1
Textural and catalytic properties of the samples[a]

Samples	d_{100} (nm)	Unit cell dimension a_0 (nm)	Pore size (nm)	Wall thickness (nm)	Micropore volume ($cm^3 g^{-1}$)	Surface area ($m^2 g^{-1}$)	Conversion of reactant (%)
M-MCM-41	4.52	5.22	2.78	2.44	0.05	919.98	44.49
MCM-41	3.77	4.35	2.95	1.40	—	957.75	11.84
Mordenite	—	—	—	—	—	—	39.74

[a]The SiO_2/Al_2O_3 ratio in all samples is 30. The wall thickness was calculated as: a_0-pore size ($a_0 = 2d(100)/3^{1/2}$).

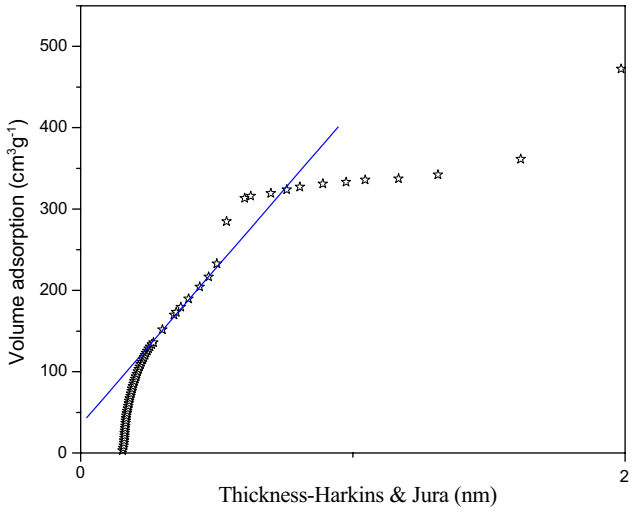

Fig. 3. *t*-plot of calcined M-MCM-41.

space to connect to each other. Apparently, the thicker mesoporous walls makes it easier for zeolite Mordenite secondary building units to be fixed in the walls. Furthermore, we observed that the pore-size distribution of the M-MCM-41 sample is somewhat broader than that of the MCM-41 sample, despite the fact that the maximum values are similar. It is proposed that this phenomenon can also be attributed to the difference between the zeolite secondary building units used for M-MCM-41 and the non-structured silicon species used for MCM-41. The stronger rigidity and larger volume of the Mordenite units makes assembly with the template relatively difficult, and this results in some disorder in the products.

Fig. 3 shows *t*-plot of calcined M-MCM-41. Generally, the *t*-plot of mesoporous material passes zero of axis, meaning no micropores in them. However, calcined M-MCM-41 does not pass zero of axis, giving the micropore volume at $0.05\,cm^3\,g^{-1}$ although the microporosity of M-MCM-41 is a little. Reasonably, the existence of micropore volume in M-MCM-41 might come from the undissolved zeolite Mordenite or be related to the recrystallization of Mordenite secondary building units.

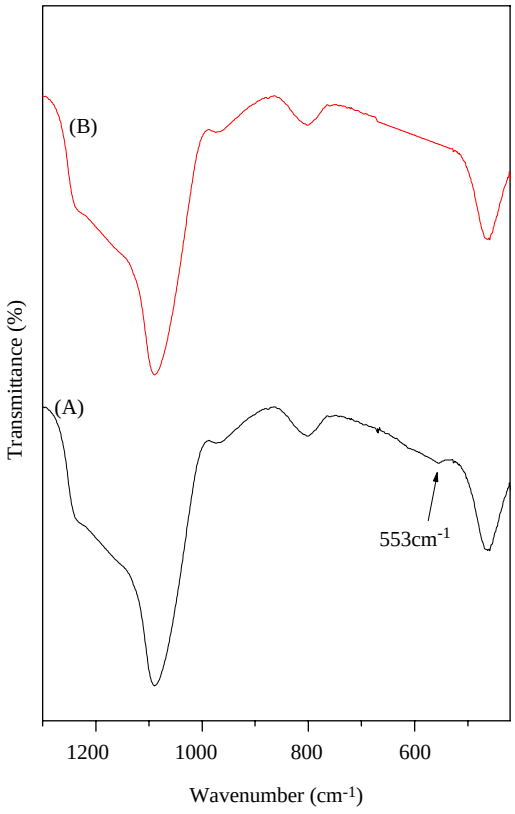

Fig. 4. IR Spectra of calcined: (A) M-MCM-41 and (B) MCM-41.

3.3. IR spectroscopy

Fig. 4 displays IR spectra of calcined M-MCM-41 and MCM-41. IR spectrum of MCM-41 shows a broadband at $460\,cm^{-1}$ in the region of 400–$600\,cm^{-1}$, which is similar to those of amorphous materials. However, M-MCM-41 exhibits an obvious band at near $550\,cm^{-1}$ in addition to the band at $460\,cm^{-1}$, which is similar to that of the five-membered rings of *T–O–T* (*T* = Si or Al) in zeolite crystals [19]. These results suggest that the mesoporous walls of M-MCM-41 contain the secondary building units of zeolite Mordenite, which are well consistent with those reported in previous literatures.

3.4. DTG spectroscopy

The experimental results of DTG analysis of the M-MCM-41 and MCM-41 are shown in Fig. 5. The two maxima of the peaks at 532 and 641 K on the DTG curve of the MCM-41 are assigned to the Hofmann decomposition of CTAB [20,21]. However, the DTG curve of the M-MCM-41 is quite different from that of the MCM-41 sample. The decomposition peaks of CTAB inside the mesopore of the M-MCM-41 shift to lower temperatures 516 and 638 K, respectively, compared with those of the MCM-41 sample. It may be suggested that the easy thermal desorption or decomposition of CTAB is due to a minor interaction between CTAB and the initially crystallized mesopore walls. This result is also in good agreement with the above discussions of mesoporous walls and IR spectra of M-MCM-41 and MCM-41.

3.5. Hydrothermal stability

Recently, hydrothermal stability of mesoporous materials has been paid much attention due to the request in industrial application, and several successful methods for improving the hydrothermal stability are used such as increasing thickness of mesoporous walls, mesoporous walls containing zeolite primary and secondary building units and increasing the level of silica condensation degree. In this work, as compared with that of MCM-41, the high hydrothermal stability of M-MCM-41 is assigned to the following two factors: (1) thicker mesoporous walls; (2) zeolite-like secondary building units in mesoporous walls. Both factors are well confirmed by experimental results.

As observed in Fig. 1 and Table 1, it is obvious that the wall thickness of M-MCM-41 is much larger than MCM-41. Additionally, amorphous nature of mesoporous walls is one of the most important factors for relatively low hydrothermal stability of mesoporous materials [22]. Obviously, introduction of zeolite secondary building units into mesoporous walls improves the hydrothermal stability of mesoporous materials significantly. M-MCM-41 exhibits a clear band at near 550 cm^{-1} (Fig. 4), confirming the existence of zeolite Mordenite secondary building units in mesoporous walls of M-MCM-41.

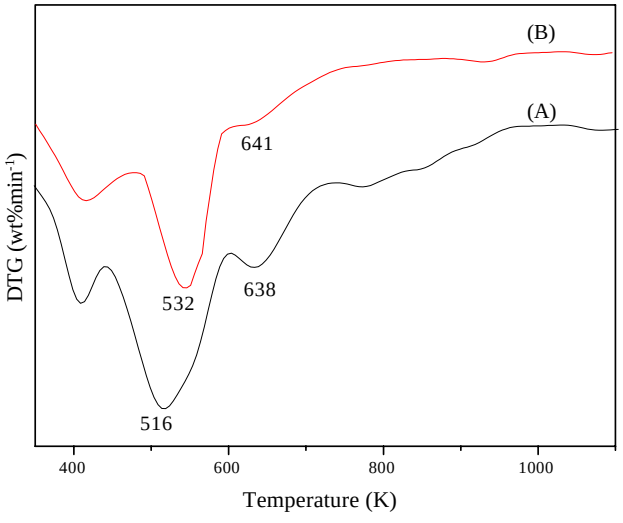

Fig. 5. DTG data of: (A) M-MCM-41 and (B) MCM-41.

3.6. Catalytic activity

The catalytic activity in the dealkylation of $C10^{+}$ aromatic hydrocarbon over Mordenite, M-MCM-41 and MCM-41 are summarized in Table 1. The conversion for the H-Mordenite (39.74%) is somehow lower than that for the H-M-MCM-41 (44.49%) due to its relatively small pore size and the large diameter of the reactant molecules. Still, the conversion for the H-M-MCM-41 (44.49%) is much higher than that for the H-MCM-41 (11.84%) sample, and this result would be ascribed to the introduction into the M-MCM-41 mesopore wall a lot of secondary building units characteristic of zeolite Mordenite which gives rise to the higher hydrothermal stability and more strong acid sites. In a word, the M-MCM-41 combines the advantages of both Mordenite (strong acidity) and MCM-41 (large pores), which makes it promising for use in future catalytic applications.

4. Conclusions

Through a two-step procedure, mesoporous molecular sieve (M-MCM-41) with pore walls of zeolite structure was successfully synthesized from the assembly of dissolved Mordenite gel with CTAB surfactant micelle, in which the zeolite Mordenite was dissolved into alkaline solution of certain concentration to produce secondary structural building units. We propose that the highly hydrothermal stability and good catalytic activity of M-MCM-41 arise from the presence of Mordenite structure building units in the mesoporous walls. This synthesis method for the hydrothermally stable mesoporous materials would be illuminating for preparing many mesoporous molecular sieves from various zeolites under alkaline or acidic conditions.

Acknowledgments

This work was supported by the National Natural Science Foundation of China (Grant No. 20173039), National Basic Research Program of China (Grant No. 2004 CB 217806), and the Petrochina Chemical Company Limited.

References

[1] C.T. Kresge, M.E. Leonowicz, W.J. Roth, J.C. Vartull, J.S. Beck, Nature 352 (1992) 710–712.
[2] A. Corma, Chem. Rev. 97 (1997) 2373.
[3] Q.H. Xia, K. Hidajat, S. Kawi, J. Catal. 209 (2002) 433.
[4] M. Matsuhashi, M. Tanaka, H. Nakamura, K. Arata, Appl. Catal. A 208 (2001) 1.
[5] H.Q. Xia, K. Hidajat, S. Kawi, Chem. Commun. 2000, 2229.
[6] H.Q. Xia, K. Hidajat, S. Kawi, J. Catal. 205 (2002) 318.
[7] C.L. Chen, S. Cheng, H.P. Lin, S.T. Wong, C.Y. Mou, Appl. Catal. A 215 (2001) 21.
[8] Y. Sun, L. Zhu, H. Lu, R. Wang, S. Lin, D. Jiang, F.S. Xiao, Appl. Catal. A 237 (2002) 21.
[9] R. Mokaya, J. Am. Chem. Soc. 124 (2002) 10636.
[10] Y. Liu, W. Zhang, T.J. Pinnavaia, Angew. Chem., Int. Ed. 40 (2001) 1255.
[11] Z. Zhang, Y. Han, L. Zhu, R. Wang, Y. Yu, S. Qiu, D. Zhao, F.S. xiao, Angew. Chem., Int, Ed. 40 (2001) 1258.
[12] Y. Han, S. Wu, Y. Sun, D. Li, F.S. Xiao, J. Liu, X. Zhang, Chem. Mater. 14 (2002) 1144.
[13] Y. Liu, W. Zhang, T.J. Pinnavaia, J. Am. Chem. Soc. 122 (2000) 8791.
[14] Y. Liu, W. Zhang, T.J. Pinnavaia, Angew. Chem., Int. Ed. 40 (2001) 1255.
[15] Y. Liu, T.J. Pinnavaia, Chem. Mater. 14 (2002) 3.
[16] Y. Han, F.S. Xiao, S. Wu, Y. Sun, X. Meng, D. Li, S. Lin, F. Deng, X. Ai, J. Phys. Chem. B 105 (2001) 7963.
[17] F.S. Xiao, Y. Han, Y. Yu, X. Meng, M. Yang, S. Wu, J. Am. Chem. Soc. 124 (2002) 888.
[18] J. Garcia-Martinez, J.Y. Ying, Abstracts of the 14th International Zeolite Conference, Cape Town, South Africa, 2004, p. 203.
[19] P.A. Jacobs, E.G. Derouane, Weitkamp, J. Chem. Soc., Chem. Commun. 12 (1981) 591.
[20] J.S. Beck, J.C. Vartuli, W.J. Roth, M.E. Leonowicz, C.T. Kresge, K.D. Schmitt, C.T.-W. Chu, D.H. Olsen, E.W. Sheppard, S.B. Mccullen, J.B. Higgins, J.L. Schlenker, J. Am. Chem. Soc. 114 (1992) 10834.
[21] X. Chen, L. Huang, G. Ding, Q. Li, Catal. Lett. 44 (1997) 123.
[22] A. Corma, Chem. Rev. 97 (1997) 2373.